The Journal of Experimental Biology 208, 3581-3591
Published by The Company of Biologists 2005
doi:10.1242/jeb.01776

Allometric scaling of flight energetics in Panamanian orchid bees: a comparative phylogenetic approach

Charles-A. Darveau[1,*], Peter W. Hochachka[1,†], Kenneth C. Welch, Jr[2], David W. Roubik[3] and Raul K. Suarez[2]

[1]*Department of Zoology, University of British Columbia, Vancouver, BC, Canada, V6T 1Z4,* [2]*Department of Ecology, Evolution and Marine Biology, University of California Santa Barbara, Santa Barbara, CA 93106-9610, USA* and [3]*Smithsonian Tropical Research Institute, Balboa, Republic of Panama*

*Author for correspondence (e-mail: darveau@zoology.ubc.ca)

†Deceased

Accepted 6 July 2005

Summary

The relationship between body size and flight energetics was studied in the clade of tropical orchid bees, in order to investigate energy metabolism and evolution. Body mass, which varied from 47 to 1065 mg, was found to strongly affect hovering flight mass-specific metabolic rates, which ranged from 114 ml CO_2 h^{-1} g^{-1} in small species to 37 ml CO_2 h^{-1} g^{-1} in large species. Similar variation of wingbeat frequency in hovering flight occurred among small to large species, and ranged from 250 to 86 Hz. The direct relationship between such traits was studied by the comparative method of phylogenetically independent contrasts (PIC), using a new molecular phylogeny generated from the cytochrome *b* gene partial sequences. We found wingbeat frequency variation is satisfactorily explained by variation in wing loading, after corrections for body mass and phylogeny. The correlated evolution of mass-specific metabolic rate, wingbeat frequency and wing loading was also revealed after correcting for phylogeny and body mass. Further, the effect of body size on flight energetics can be understood in terms of a relationship between wing form and kinematics, which directly influence and explain the scaling of metabolic rate in this group of bees.

Key words: metabolic rate, evolution, allometry, wingbeat frequency, wing loading, phylogenetically independent contrasts, orchid bee.

Introduction

Flying insects achieve some of the highest rates of aerobic energy metabolism in the animal kingdom (Sacktor, 1976; Suarez, 2000). The development of asynchronous flight muscles was a major evolutionary innovation that contributed to the impressive flight abilities and evolutionary success of many insect species. Decoupling the muscle activation and contraction systems permitted the extraordinarily high muscle contraction frequencies. However, even asynchronous flyers display a wide range in flight performance, often involving finer evolutionary adjustments in form and function. One group of asynchronous flyers, the orchid bees (Apidae: Euglossini), includes 200 described species in the tropical Americas (Cameron, 2004; Roubik and Hanson, 2004). In a series of pioneering studies, Casey et al. (1985) exploited the species size variation among co-occurring orchid bees to investigate allometric scaling of flight biomechanics and energetics. They found that mass-specific metabolic rates and wingbeat frequencies both decline with increasing body mass. Nevertheless, body mass alone did not fully account for species variation in metabolic rate or wingbeat frequency. This led Casey et al. (1985) to propose that characters associated with phylogeny must be partly responsible for the observed variation in species traits. The orchid bees, therefore, represent an excellent opportunity to examine the interplay of morphology, kinematics and energetics in the context of phylogenetic relationships (Felsenstein, 1985; Garland et al., 1992; Harvey and Pagel, 1991).

Phylogenetic information is often incorporated into analysis of continuous traits by using a hypothesized tree topology and associated branch lengths (Garland et al., 1992). In this study, we present a new phylogenetic hypothesis for orchid bees based on the cytochrome *b* gene (*cyt b*) partial sequences, and use it to analyze metabolic rate evolution. Using phylogenetically independent contrasts (PIC), we analyze the correlated evolution of body mass, wing morphology, wingbeat frequency, and the energetic cost of hovering flight. This range of data provides a new framework for the understanding of evolutionary relationships between species size and metabolism.

Materials and methods

Study site and orchid bee collection

The 32 species used to generate the molecular phylogeny were

collected at various sites in Panama by David W. Roubik and were either preserved in ethanol or frozen (–80°C). Data on flight energetics were obtained from 86 individuals of 18 species, representing a subset of the 32 species included in the molecular phylogenetic work. Measurements were conducted during the transition from dry to wet season in June 2003 near the center of the 15 km^2 island of Barro Colorado, in the Panama Canal, at ambient temperatures of 25–30°C. Only male orchid bees were used, as these could be attracted and caught using chemical lures as described in the accompanying paper (Suarez et al., 2005).

Molecular phylogeny

To assess the phylogenetic relatedness of the various species used, we generated hypothetical phylogenies based on partial sequences for the mitochondrial gene *cyt b*. We extracted total DNA from individuals of 32 species, mainly from the thorax (sometimes including legs), using the DNeasy DNA extraction kit (Qiagen, Mississauga, ON, Canada), following the manufacturer's recommended homogenization procedure for insects.

The amplification procedure used was modified from Koulianos and Schmid-Hempel (2000). Using their *cyt b* primers, we amplified a 716 bp fragment. The conditions that yielded the highest amplification success for most species were as follows: denaturation at 94°C for an initial 2 min and then 40 cycles of 1 min denaturation at 94°C, annealing at 43°C for 1 min, extension at 72°C for 1 min, followed by a 5 min final extension (Perkin-Elmer DNA Thermal Cycler, Woodbridge, ON, Canada); *Taq* polymerase 2.5 U (Invitrogen, Burlington, ON, Canada), $MgCl_2$ 1.5 mmol, dNTP 0.2 mmol, primers 0.5 μmol l^{-1}. For some species, the yield of amplification product was low. This required slight modification of time, temperature, $MgCl_2$ and *Taq* concentrations. DNA product was purified using Quiaquick purification columns (Qiagen). Sequencing was performed by the University of British Columbia Nucleic Acid and Protein Sequencing Unit using an ABI 377 automated sequencer. The primers used for sequencing were the same as those used for amplification. In most cases, one individual was sufficient to provide a sequence.

The *cyt b* sequences (~650 bp) obtained for 32 species were aligned using ClustalX. Sequences were also obtained from GenBank for *Eulaema meriana* (GenBank accession number AF181614), *El. bombiformis* (AF002728), *Eufriesea caerulescens* (AF181613), in addition to the selected outgroups: *Xylocopa virginica* (AF181618), *Apis mellifera* (NC_001566), *Bombus hyperboreus* (AF066968), *Trigona hypogea* (AF181617) and *Melipona bicolor* (NC_004529). Trees were rooted with *Xylocopa virginica*, which is hypothesized to be a sister clade (Ascher and Danforth, 2001).

Aligned sequences were imported into PHYML for maximum likelihood analysis. Several sequence divergence models were executed, and a general time reversal with gamma distribution was selected based on log-likelihood score. The support for the nodes was obtained with 1000 bootstrap replicates using PHYML and SEQBOOT and CONSENS from PHYLIP 3.57c (Felsenstein, 1995). Additional analyses were performed with the neighbor-joining distance method using MEGA version 2.1 (Kumar et al., 2001), and Bayesian analysis using MrBayes 3.0 (Huelsenbeck and Ronquist, 2001).

Respirometry and wingbeat frequency measurements

Rates of CO_2 production ($\dot{V}_{CO_2}$ values) were measured as described in the accompanying paper (Suarez et al., 2005) using a FOX flow-through field respirometry system equipped with a Sable Systems (Henderson, NV, USA) CA-2A CO_2 analyzer. Smaller species, up to 400 mg in body mass, were flown in a 0.5 l flask with sidearm, while a similar flask of 1 l capacity was used for larger species. Air was drawn into the flasks through perforated rubber stoppers and out through the sidearms through Tygon tubing at a rate of 1.5 l min^{-1}. Orchid bees, like honeybees (Crabtree and Newsholme, 1972; Rothe and Nachtigall, 1989) fuel flight exclusively by carbohydrate (Suarez et al., 2005). Therefore, the $\dot{V}_{CO_2}$ values measured are equivalent to rates of O_2 consumption ($\dot{V}_{O_2}$), i.e. RQ=1 (Suarez et al., 2005). Data acquisition and analysis were performed using Datacan (Sable Systems).

Wingbeat frequency measurements were performed simultaneously using an optical flight detector (Qubit systems, Kingston, ON, Canada), positioned beneath the respirometry chambers. The instrument was linked to a portable computer and the signal was acquired and analyzed using Trex (Qubit systems). The wingbeat of an insect performing hovering flight in the chamber was detected by the photocell. Intervals of 2 s were analyzed for fundamental frequency and data for each individual were averaged for the initial 30 s of flight.

Wing morphology

The individuals were frozen on dry ice, stored at –80°C, and brought to the laboratory for morphological measurements. From each individual, one pair of wings was removed and flattened between microscope slides. A digital image of the wings on a 1 cm grid background was taken for image analysis using Scion image.

Data analysis

All data are presented as species means ± S.D. (standard deviations) of individual measurements. However, both individual data and species means were analyzed. The effect of body mass M_b on the different characters was tested using the least-squares linear regression performed on log-transformed data to obtain the power equation $Y=aM_b^b$. Further analyses of wingbeat frequencies and mass-specific metabolic rates were performed using stepwise regressions to test the relative importance of body mass, forewing length, total wing area and wing loading. In addition, we corrected for body mass covariation using an analysis of residuals.

Analysis of phylogenetically independent contrasts was conducted using the PDAP (Midford et al., 2003) module in Mesquite (Maddison and Maddison, 2004). Standardized independent contrasts were obtained from the log-transformed character data, and presented using the maximum likelihood tree obtained from *cyt b* sequence information (Fig. 1). This

phylogenetic tree was pruned to include only the 12 species from which a complete set of flight data was obtained (Fig. 2). We also performed all analyses using the hypothesized trees obtained from our other phylogenetic analyses (neighbor-joining, Bayesian, maximum parsimony). The results of these analyses were qualitatively the same (data not shown). To further evaluate phylogenetic tree topology and branch length uncertainty (see Garland et al., 1992, 1993; Martins and Housworth, 2002), we implemented our analysis of character data using 10 000 trees generated from a Bayesian analysis and reported the correlation coefficient frequency distribution of standardized independent contrasts using Mesquite. The same analysis performed with 10 000 simulated trees yielded the same results (not shown). We analyzed the relationship among independent contrasts with the same series of tests we used for the conventional analysis. We first tested body mass scaling effects on the different characters, using least-squares linear regression through the origin performed to analyze standardized contrasts (Garland et al., 1992). We then carried out stepwise regression through the origin to analyze the independent contrasts of wingbeat frequency and mass-specific metabolic rate, to test for the effects of body mass, forewing length, total wing area and wing loading. Finally we statistically controlled for body mass using the residuals obtained from the independent contrasts body mass regressions, and plotted the residuals and tested for regression through the origin (Garland et al., 1992). All analyses were performed first using a model of gradual evolution, where characters usually experience greater changes along longer branches (Garland et al., 1993). We ensured that branch lengths adequately standardized the

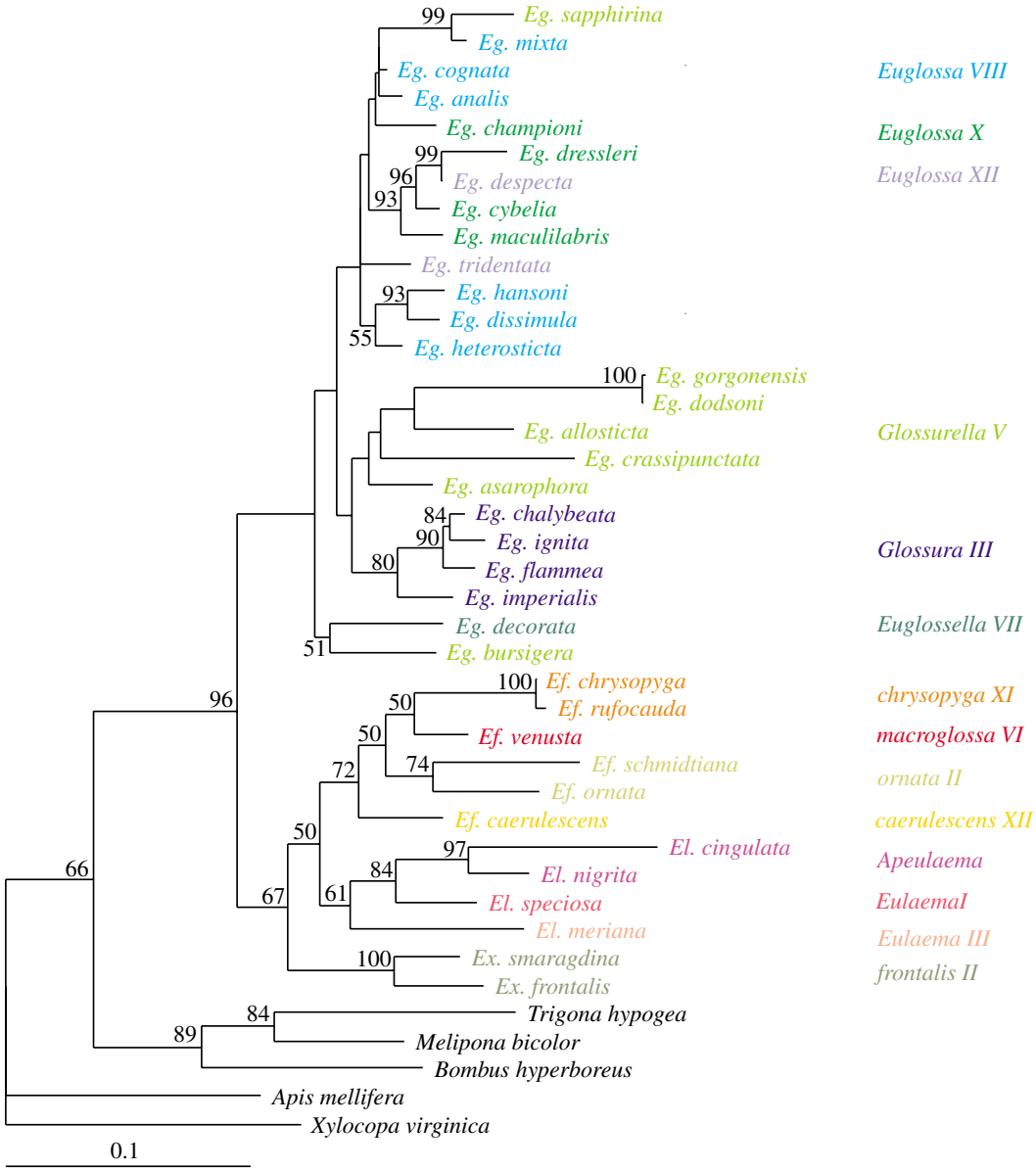

Fig. 1. Phylogenetic tree hypothesized for 36 orchid bee (Apidae: Euglossini) species, based on *cyt b* partial sequences and inferred using the maximum likelihood method. Node bootstrap support values greater than 50% are shown. Species groupings, based on Cameron (2004), are presented in different colors. *Eg*., *Euglossa*; *Ef*., *Eufriesea*; *Ex*., *Exaerete*; *El*., *Eulaema*.

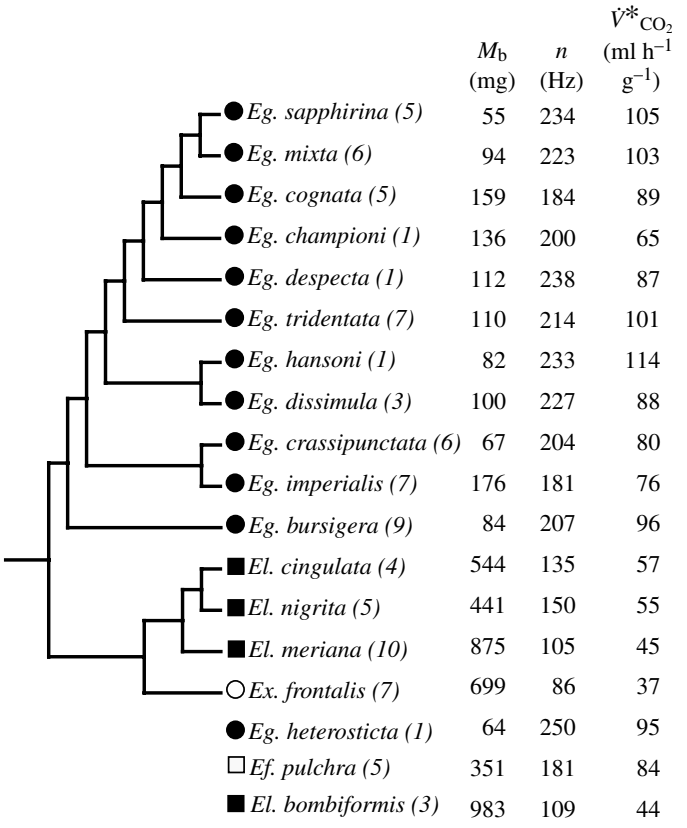

Fig. 2. Phylogenetic relationships among 15 of 18 species of orchid bees used for hovering flight measurements. The character values are presented for body mass M_b, wingbeat frequency n, mass-specific metabolic rate $\dot{V}^*_{CO_2}$. Sample size, N, is identified for each species in parentheses.

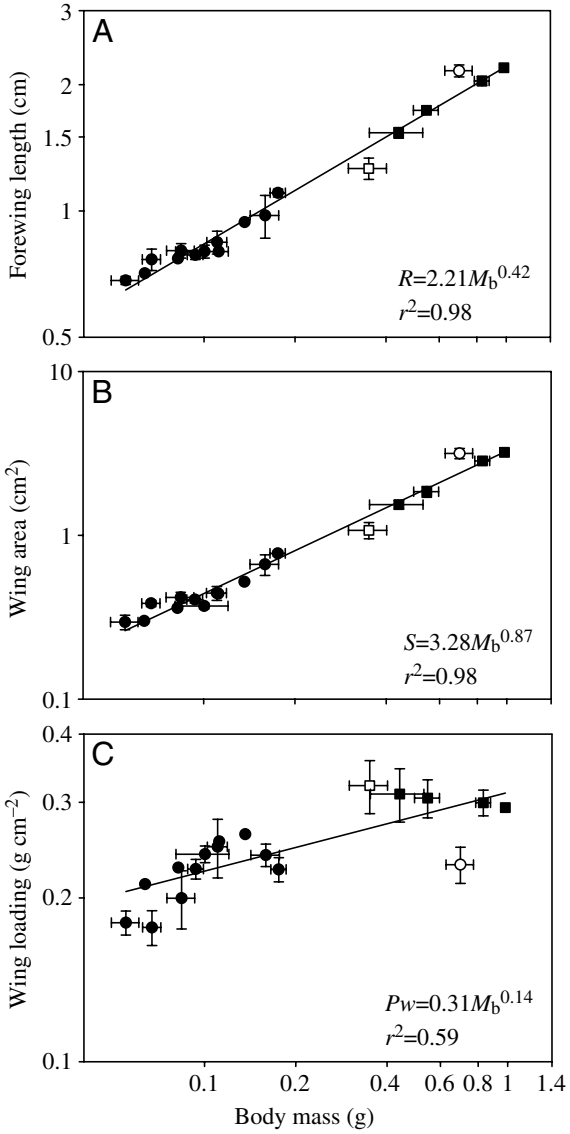

Fig. 3. Relationships between body mass M_b and wing morphological characters. (A) Forewing length R, (B) total wing area S and (C) calculated wing loading Pw. Solid circles represent the genus *Euglossa*; open circles, *Exaerete*; filled squares, *Eulaema*; open squares, *Eufriesea*.

contrasts by plotting the absolute value of standardized independent contrasts and their standard deviation (Garland et al., 1992). The raw branch lengths obtained from *cyt b* genetic distances were used, but several branch length transformations (Grafen, Pagel, Nee, logarithmic) were also tested and yielded the same results (not shown). A speciational model of evolution, where changes occur with a speciation event, was simulated by setting all branch lengths to 1 (Garland et al., 1993).

Results

Molecular phylogeny

We aligned 653 base pairs from the amplified sequence (GenBank accession number AY916090-AY916122). The nucleotide frequency had a strong A/T bias (A=0.357, T=0.446, C=0.104, and G=0.093). The uncorrected p-distance obtained from pairwise comparison of nucleotide sequences ranged from 0.4% between *Ef. chrysopyga* and *Ef. rufocauda*, to 20% between *Eg. sapphirina* and *El. cingulata* (not shown).

Although ten sequences were incomplete and seven sequences taken from GenBank were partially overlapping (550 bp), the aligned sequences were sufficient to yield a hypothetical phylogeny (Fig. 1). This maximum likelihood tree was obtained using the general time reversal (GTR) model with gamma distribution (α=0.501), with node support indicated by the bootstrap value. In the *Euglossa*, nodes were supported near the crown species, but deeper nodes in that clade were poorly resolved. The genera *Eulaema* and *Eufriesea* appeared to form a clade which was not supported with high bootstrap values. Nonetheless, the topology obtained with neighbor-joining and Bayesian methods (not shown) always grouped the two genera. The *cyt b* information places *Exaerete* as the sister genus of the *Eulaema–Eufriesea* group. Finally, the *Euglossa* genus was resolved as sister of the other genera. Alternative methods of phylogenetic inference and genetic distance methods yielded similar topologies with nodes with bootstrap values greater than 50% generally conserved (results not shown).

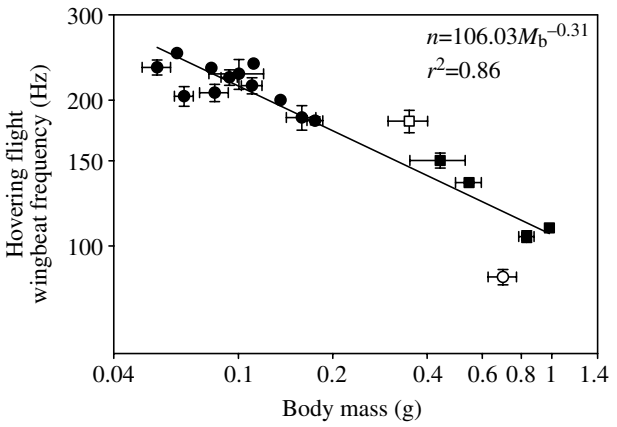

Fig. 4. Relationship between body mass and hovering flight wingbeat frequency. Symbols as in Fig. 3.

Morphology

The relationship between body mass and wing morphology measurements was assessed in 18 species of euglossine bees. Body mass ranged from 47 mg (*Eg. sapphirina*) to 1065 mg (*El. bombiformis*). The relationship between body mass and all variables described below is expressed as power functions of the form, $Y=aX^b$. Thoracic mass is a constant proportion (43%) of body mass (results not shown). Forewing length and total wing area were related to body mass to the power 0.42 (95% CL: 0.38, 0.46) and 0.87 (95% CL: 0.80, 0.94) respectively (Fig. 3A,B). In agreement with the wing area allometry, the calculated wing loading was higher in larger species, scaling with an exponent of 0.14 (95% CL: 0.08, 0.21) (Fig. 3C). The analyses performed using PIC show that the body mass effect remained significant using the phylogeny in Fig. 1 or the simulated trees (not shown). The allometric exponents obtained using PIC and gradual evolution from Fig. 1 were 0.40 (95% CL: 0.34, 0.47), 0.87 (95% CL: 0.72, 1.02) and 0.16 (CL: 0.03, 0.29) for wing length, wing area and wing loading, respectively.

Wingbeat frequency

The relationship between body mass and wingbeat frequency during hovering flight is presented in Fig. 4. Frequencies ranged from 86 (*Ex. frontalis*) to 250 Hz (*Eg. heterosticta*). Species body mass accounted for a considerable portion (r^2=0.88) of the threefold variation in wingbeat frequency, and the scaling exponent was –0.31 (95% CL: –0.24, –0.37; Fig. 4). Wing area and length, however, were related to wingbeat frequency with a greater coefficient of determination (Table 1).

Analyses of body mass relationship with wingbeat frequency performed using PIC are presented in Table 1 and Fig. 5. When the hypothesized phylogeny in Fig. 1 was applied, the body mass effect remained highly significant under both gradual and speciational models of character evolution (Table 1). The exponent was similar to that obtained from conventional analysis, with –0.30 (CL: –0.18, –0.43) for gradual and –0.30 (CL: –0.17, –0.43) for speciational. The uncertainty of the hypothesized phylogeny was tested by analysis of the contrasts between body mass and wingbeat frequency using 10 000 different trees obtained by Bayesian analysis. The resulting frequency distribution indicated that wingbeat frequency and body mass evolution were closely correlated (Fig. 5). The average correlation coefficient of the distribution was 0.86, and the values obtained from the *cyt b* tree in Fig. 1 were 0.87 and 0.85 for gradual and speciational evolution, respectively (Table 1 and Fig. 5A).

Metabolic rate

The metabolic rates during hovering flight ranged from 5.4 (*Eg. crassipunctata*) to 43.2 ml CO_2 h^{-1} (*El. bombiformis*) and scaled against body mass with an exponent of 0.68 (95% CL: 0.60, 0.77) (Fig. 6A). Mass-specific rates of CO_2 production ranged from 37.4 to 114.4 ml CO_2 h^{-1} g^{-1}, in *Ex. frontalis* (699 mg) and *Eg. hansoni* (82 mg), respectively, scaling with an exponent of –0.31 (95% CL: –0.40, –0.23; Fig. 6B). Analysis of relationships among mass-specific metabolic rates, wingbeat frequencies and morphometric parameters determined that wingbeat frequency explained most of the variation in metabolic rate, but wing length and area also had higher coefficients of determination than body mass (Table 2).

Incorporating phylogenetic information (Fig. 1) into the analysis confirmed the relationships presented above, in which mass-specific metabolic rate was accounted for chiefly by wingbeat frequency, followed by wing length and area, and then by body mass. Analyzing the effect of body mass on mass-

Table 1. *Relationship between wingbeat frequency and body morphometrics of euglossine bees using conventional and phylogenetically independent contrasts (PIC) analyses*

	Conventional			PIC gradual			PIC speciational		
Parameter	Equation	r^2	P	b	r^2	P	b	r^2	P
M_b (g)	$106M_b^{-0.31}$	0.862	<0.001	–0.30 (–0.18, –0.43)	0.756	<0.001	–0.30 (–0.17, –0.43)	0.723	<0.001
R (cm)	$188R^{-0.75}$	0.933	<0.001	–0.80 (–0.59, –1.00)	0.885	<0.001	–0.78 (–0.55, –1.01)	0.853	<0.001
S (cm^2)	$160S^{-0.36}$	0.937	<0.001	–0.37 (–0.28, –0.46)	0.899	<0.001	–0.38 (–0.28, –0.48)	0.874	<0.001
Pw (g cm^{-2})	$52Pw^{-0.88}$	0.246	0.036		0.046	NS		0.042	NS

N=18 species for conventional analysis and 11 contrasts for PIC analysis.
For gradual evolution, branch lengths from Fig. 1 were used and for speciational model, branch lengths were set to 1.
M_b, body mass; R, forewing length; S, total wing area; Pw, calculated wing loading; NS, not significant.

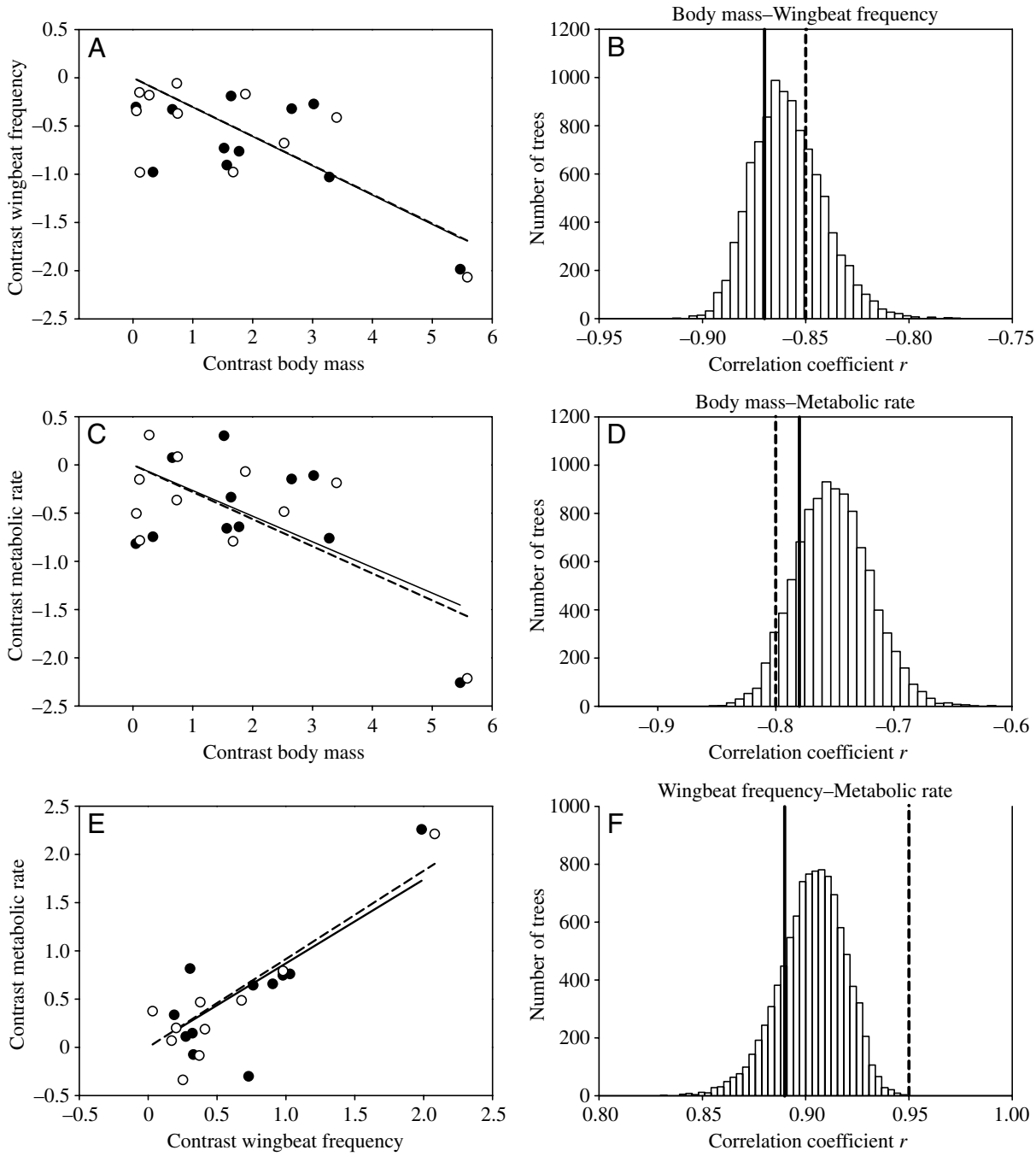

Fig. 5. (A,C,E) Relationship between body mass, wingbeat frequency and mass-specific metabolic rate independent contrasts obtained from *cyt b* phylogeny (Fig. 1), and using gradual (filled circles, solid lines) and speciational (open circles, broken lines) models of character evolution. (B,D,F) These relationships (solid and broken lines) are superimposed on the distribution of correlation coefficients resulting from analyses performed with 10 000 different trees (see Materials and methods).

specific metabolic rate yielded similar exponents for gradual (–0.27 CL: –0.11, –0.42) and speciational evolution (–0.28 CL: –0.14, –0.43). A test for phylogenetic uncertainty (Fig. 5B), revealed a significant average correlation coefficient, 0.76, while the values obtained using the phylogeny in Fig. 1 were 0.78 and 0.80 for gradual and speciational evolution, respectively (Table 2 and Fig. 5B).

Morphology, wingbeat frequency and metabolic rate

To analyze the interrelationships between the body mass, wing morphology, wingbeat frequency and metabolic rate, we first performed stepwise regressions. For wingbeat frequency, wing area was introduced in the regression model, and much of the remaining variation was explained by wing loading. Moreover, using any of the three variables associated with size

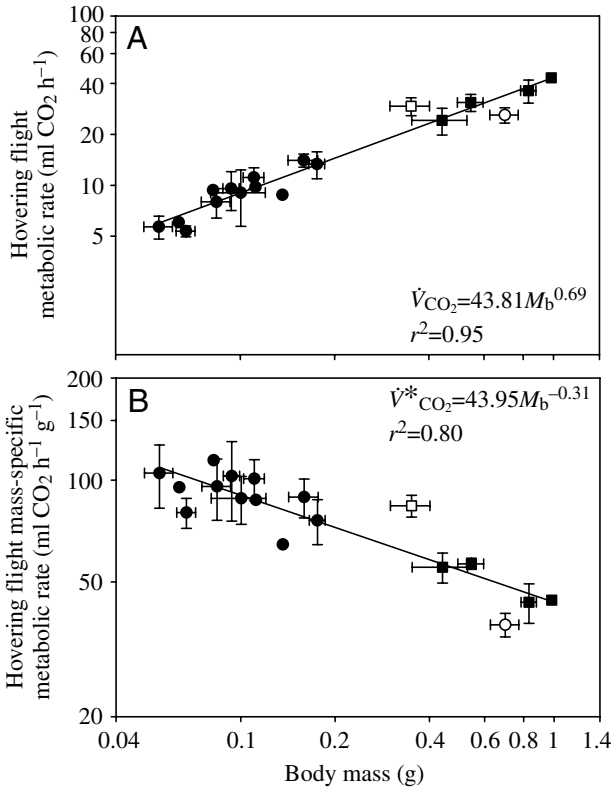

Fig. 6. Relationships between body mass and hovering flight whole-animal (A) and mass-specific (B) metabolic rate. Symbols as in Fig. 3.

(body mass, wing length, wing area), and wing loading, the coefficient of determination of the model was 98%. Stepwise regression analysis of mass-specific metabolic rate introduced wingbeat frequency alone in the model. Performing these analyses using PIC produced the same qualitative results. In addition, the wingbeat frequency and metabolic rate relationship was analyzed for uncertainty (Fig. 5C), and a high average correlation coefficient was observed (r=0.90), comparable to those observed with our *cyt b* phylogeny (0.89 and 0.95 for gradual and speciational evolution).

The functional relationships among the variables were further analyzed by examining residuals obtained from the body mass relationship, i.e. as body mass corrected variation. The wingbeat frequency residual variation was largely explained (r^2=0.86) by residual variation in wing loading (Fig. 7A). The residuals obtained for wing length and wing area also had strong correlations (not shown), indicating that a species of a given mass with longer wings or wings of greater area had lower wingbeat frequency; i.e. there was positive correlation between wing loading and wingbeat frequency. The same analyses performed using residuals obtained from the contrast values for gradual and speciational evolution also yielded strong positive correlations between wingbeat frequency and wing loading (Fig. 7B).

The body mass corrected relationship between hovering flight mass-specific metabolic rate and wingbeat frequency was significant and positive (Fig. 8A). At one end of the distribution, *Eufriesea pulchra* displayed high wingbeat frequency and metabolic rate for its body mass while, at the other end, *Exaerete frontalis* had a low frequency and low metabolic rate for its mass. Analysis of the residuals obtained from PIC analysis confirmed this relationship for both models of character evolution (Fig. 8B). Additionally, the conventional statistical analysis performed without *Ef. pulchra* and *Ex. frontalis* yielded the same results (not shown).

Analysis of residual variation of metabolic rate also revealed mass-corrected wing loading was positively correlated with hovering flight energy turnover (Fig. 9A). Again, *Ef. pulchra* and *Ex. frontalis* were found at opposite ends of the distribution. The relationship held upon the application of PIC analysis (Fig. 9B).

Discussion

Phylogeny of euglossine bees

The orchid bees (Euglossini) represent the only solitary tribe of the sub-family Apinae, or corbiculate bees, which also include eusocial honey bees (Apini), bumblebees (Bombini), and stingless bees (Meliponini). The origin of orchid bees is uncertain, given incongruity between hypothesized morphological and molecular relationships among tribes (Cameron, 2004; Roubik and Hanson, 2004). Within the tribe Euglossini, five genera exist, among which five hypothesized

Table 2. *Relationship between mass-specific metabolic rate, wingbeat frequency and body morphometrics of euglossine bees using conventional and phylogenetically independent contrasts (PIC) analyses*

	Conventional			PIC gradual			PIC speciational		
Parameter	Equation	r^2	P	b	r^2	P	b	r^2	P
n (Hz)	$0.41n^{1.00}$	0.887	<0.001	0.87 (0.55, 1.19)	0.787	<0.001	0.93 (0.70, 1.15)	0.895	<0.001
M_b (g)	$44M_b^{-0.31}$	0.797	<0.001	–0.27 (–0.11, –0.42)	0.601	<0.001	–0.28 (–0.14, –0.43)	0.647	<0.001
R (cm)	$79R^{-0.76}$	0.862	<0.001	–0.71 (–0.43, –1.01)	0.750	<0.001	–0.73 (–0.45, –1.01)	0.770	<0.001
S (cm^2)	$67S^{-0.37}$	0.851	<0.001	–0.32 (–0.17, –0.47)	0.699	<0.001	–0.35 (–0.22, –0.49)	0.784	<0.001
Pw (g cm^{-2})	$19Pw^{-0.98}$	0.272	0.027		0.027	NS		0.035	NS

N=18 species for conventional analysis and 11 contrasts for PIC analysis.
For gradual evolution, branch lengths from Figure 1 were used and for speciational model, branch lengths were set to 1.
n, wingbeat frequency; M_b, body mass; R, forewing length; S, total wing area; Pw, calculated wing loading; NS, not significant.

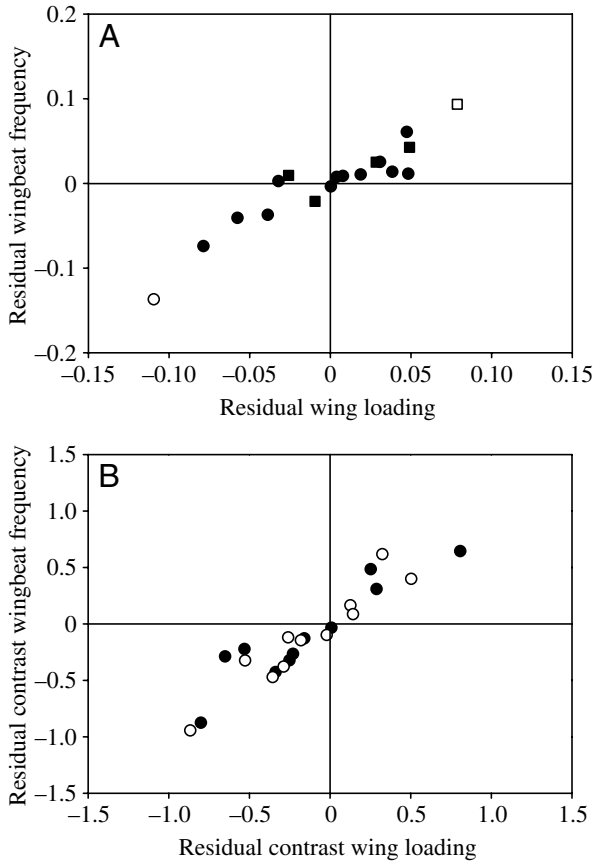

Fig. 7. Correlations between wing loading and wingbeat frequency residuals obtained from (A) the body mass regression (r^2=0.86, $F_{1,16}$=8.74, P=0.0088) and (B) from independent contrasts for gradual (filled circles, r^2=0.86, $F_{1,9}$=62.88, P< 0.0001) and speciational (open circles, r^2=0.90, $F_{1,9}$=90.94, P<0.0001) models of character evolution. Symbols in A as in Fig. 3.

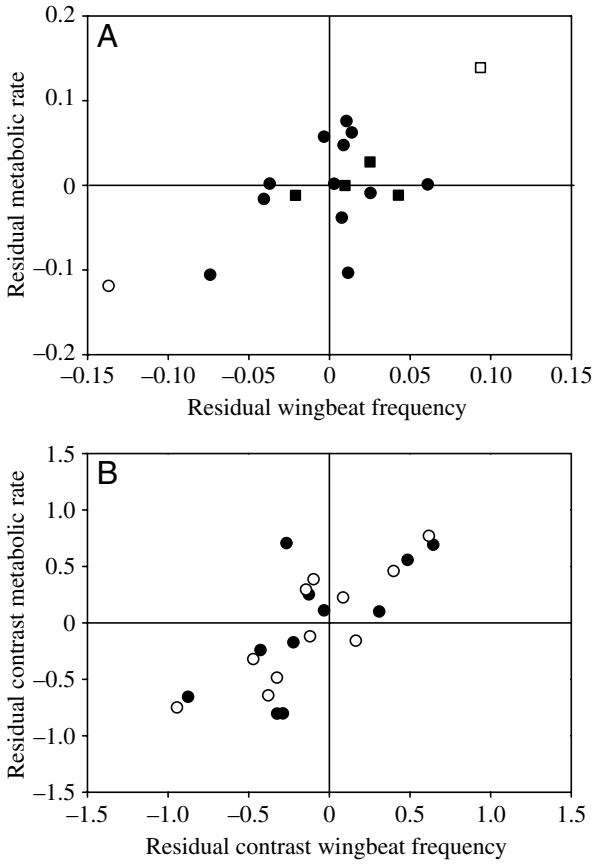

Fig. 8. Correlations between hovering flight wingbeat frequency and mass-specific metabolic rate residuals obtained from (A) the body mass regression (r^2=0.46, $F_{1,16}$=14.25, P=0.0015) and (B) from independent contrasts for gradual (filled circles, r^2=0.47, $F_{1,9}$=8.73, P=0.0144) and speciational (open circles, r^2=0.70, $F_{1,9}$=23.73, P=0.0007) models of character evolution. Symbols in A as in Fig. 3.

relationships have been proposed over the last 20 years (reviewed by Cameron, 2004). One recent analysis, using both morphological and molecular data, placed the parasite genus *Aglae* most basal, and either *Euglossa* or *Exaerete* resulted as the sister group to *Eulaema–Eufriesea* (Michel-Saltzat et al., 2004).

Prior to our work, there have been no phylogenies available at the species level for orchid bees (but see Dick et al., 2004). Our hypothesized phylogeny (Fig. 1), which includes 37 species in four genera and several subgenera, shows groups almost entirely consistent with the higher taxonomic scheme (subgenera and genera) discussed by Dressler (1978), and is at least compatible with the phylogeny suggested by Cameron (2004). Nodes near the tip of the tree are supported by high bootstrap values, while the deeper nodes are generally characterized by low values (Fig. 1). For example, the species groups classified by Dressler (1978) that are found in subgenus *Euglossa* are sometimes separated in our phylogeny, indicating that they may not derive from a common ancestor (e.g. *Euglossa* VIII, X, XII in Fig. 1). Other recent work with a number of widespread species and a CO1 marker (Dick et al., 2004) has shown reticulate evolution of species pairs, and species associations not in agreement with some previous classifications. Thus, we use our hypothesized tree with caution, because the tree topology of the orchid bees is unstable.

Body mass, wing morphology and wingbeat frequency

Our analysis of flight performance and its determinants established the linkages between wing morphology and wingbeat frequency during hovering flight. The variation in wingbeat frequency among species was explained well by their body mass (Fig. 4). This allometric relationship and the scaling exponent of –0.31 (Fig. 4) are consistent with results obtained previously by Casey et al. (1985) and, more recently, with results obtained in load-lifting experiments (Dillon and Dudley, 2004). The effect of size on wingbeat frequency can be understood in terms of the resonance properties of the flight apparatus. For a mechanically resonant system such as an asynchronous muscle, the oscillation frequency is inversely proportional to the inertial load on the system, which corresponds to the mass distribution along the wing length (Dudley, 2000). Indeed, reducing inertial load on asynchronous flight muscle by cutting short the wings increases the

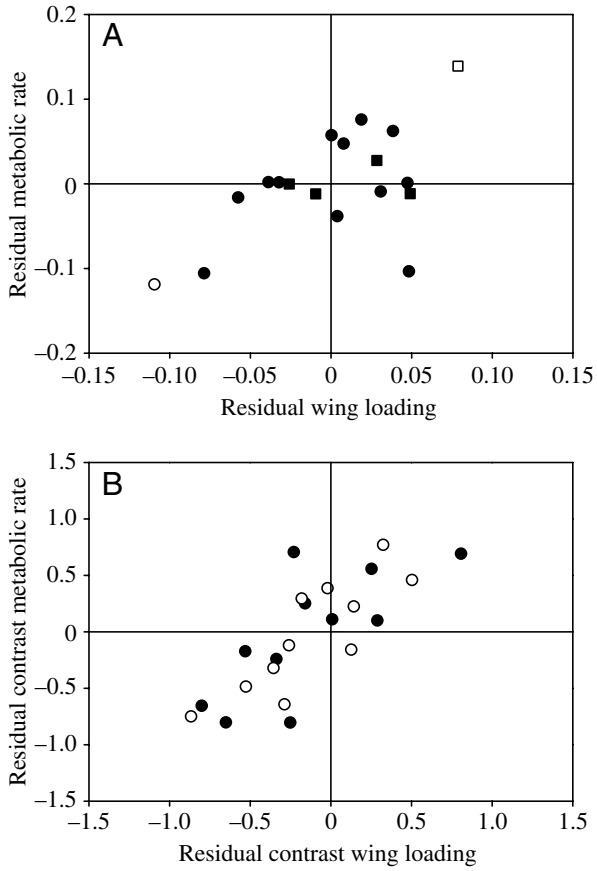

Fig. 9. Correlations between wing loading and mass-specific metabolic rate residuals obtained from (A) the body mass regression (r^2=0.34, $F_{1,16}$=8.23, P=0.0110) and (B) from independent contrasts for gradual (filled circles, r^2=0.50, $F_{1,9}$=9.89, P=0.0104) and speciational (open circles, r^2=0.66, $F_{1,9}$=19.11, P=0.0014) models of character evolution. Symbols in A as in Fig. 3.

frequency, as expected for a resonant system (Sotavalta, 1952). Thus, although body mass and wingbeat frequency are correlated, it is the wing size (length and area) that more directly influences wingbeat frequency. Such a conclusion is supported by our data showing that wing length and wing area were related to wingbeat frequency with greater coefficients of determination than was body mass (Table 1).

The relationship between wing loading and wingbeat frequency was both negative and weak (Table 1). Body mass evidently had differential effects on these two variables: a negative scaling effect on frequency but a positive one for wing loading. Together, these result in the weak negative correlation between wing loading and wingbeat frequency. Byrne et al. (1988) investigated the relationship between body mass, wing loading and wingbeat frequency in insects ranging from 3.3×10^{-5} to 2.8 g (Fig. 10). They found that wing loading and wingbeat frequency are positively correlated when data are analyzed within relatively small ranges of body size. However, when data for the entire size range are analyzed, wingbeat frequency and wing loading are no longer correlated. In the present work, we account for the confounding effects of body mass by statistical removal of its effect on wing loading and wingbeat frequency. This procedure resulted in a strong positive correlation between the two variables (Fig. 7A). Reanalysis of the data of Byrne et al. (1988) along with our euglossine data reveals the same pattern, with a high correlation coefficient (r=0.89) for the relationship between residuals (Fig. 10D). We conclude that in orchid bees and possibly among flying insects in general, wingbeat frequency is strongly related to wing loading, after controlling for covariation in body mass.

Stroke frequency and metabolic rate

Among the aerobic muscles of a given type undergoing prolonged, sustained cycles of contraction and relaxation, operating frequency is a primary determinant of power output (Pennycuick and Rezende, 1984). If myofibrillar stress and strain are considered to be independent of size, then a scaling of the energetic cost of steady-state flight would be expected to depend upon the scaling of operating frequency. Our study showed a strong, positive relationship between wingbeat frequency and metabolic power input (V_{CO_2}) during hovering flight. This strong correlation persists after controlling for both body mass and phylogenetic relatedness. The allometric relationships for wingbeat frequency and mass-specific metabolic rate yield similar exponents (Figs 4 and 6) as those obtained by Casey et al. (1985). In our study, the correlation between metabolic rate and wingbeat frequency residuals lends empirical support to the proposal that wingbeat frequency is the primary determinant of muscle power output and, therefore, metabolic rate during hovering flight.

Dudley (1995) studied hovering flight kinematics in three species of orchid bee (*Eg. dissimula*, *Eg. imperialis* and *El. meriana*) that flew in hypo-dense mixtures of helium and oxygen (heliox). Wingbeat amplitude increased from about 105° in normal air to 140° when flying in heliox. Dillon and Dudley (2004) investigated maximal load-lifting flight capacity in 11 species of orchid bees. They found that, in flight, orchid bees could sustain about twice their own body mass, and that their load lifting capacity scaled isometrically. While lifting maximum loads, wingbeat frequencies scale allometrically with an exponent similar to that during normal hovering. The wing stroke amplitudes, however, increase to approximately 140° in all species. Thus, interspecifically, stroke amplitude is conserved during normal hovering in ambient air while, intraspecifically, flight power output in response to various imposed loads can be modulated through changes in stroke amplitude. As the bees in the present study were induced to hover in ambient air without added loads, it is reasonable to assume there was a constant stroke amplitude across species.

PIC and correlated evolution

Using PIC analysis allowed incorporation of phylogenetic information to study mechanistic and statistical relationships in the data. The utility of such an approach can be appreciated by considering how markedly the body mass of species and

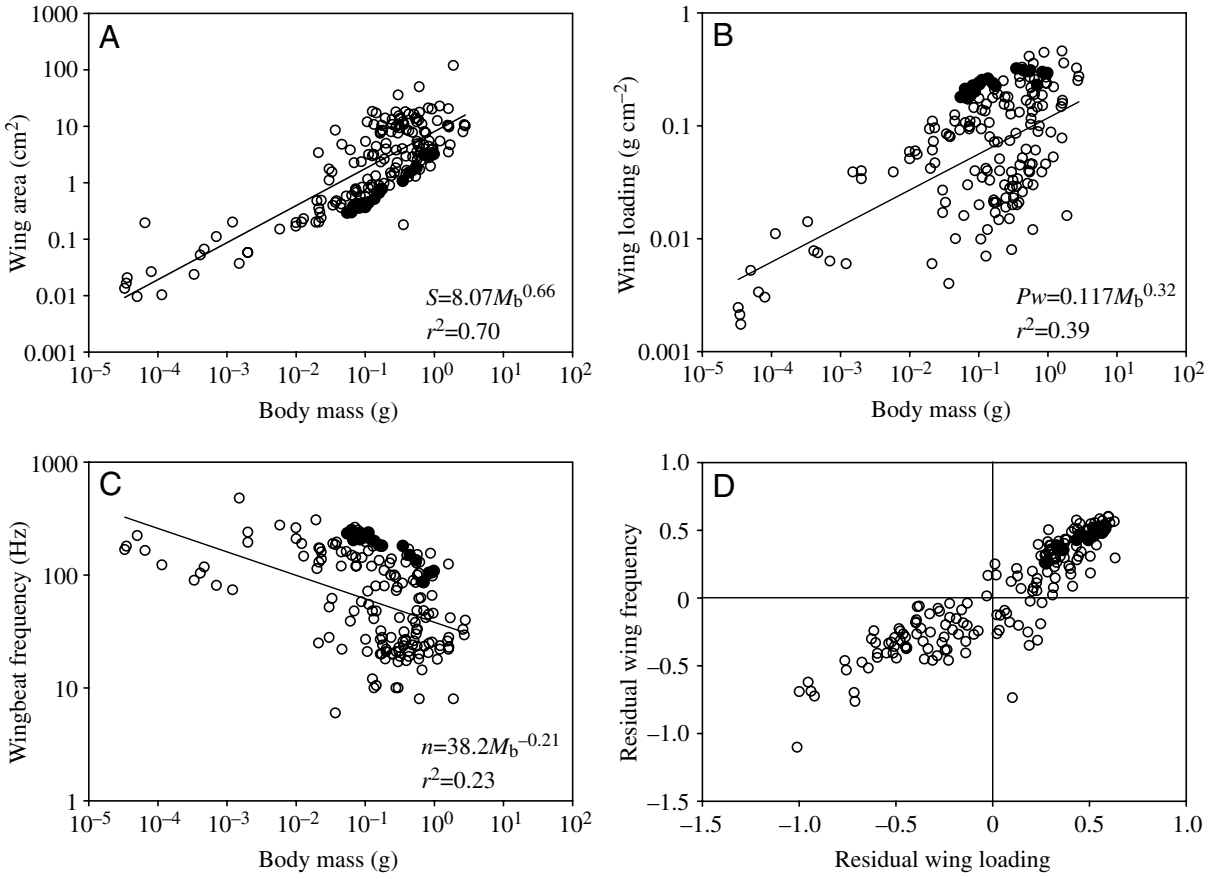

Fig. 10. Relationships between body mass and wing area (A), wing loading (B) and wingbeat frequency (C) in insects ranging from fruit flies to moths (open circles; Byrne et al., 1988) and orchid bees (filled circles; this study). (D) The correlation between wing loading and wingbeat frequency residuals obtained from the body mass regression in B and C.

correlated characters were influenced by phylogenetic group (Fig. 2). An obvious weakness of this approach is its dependence on correctness of the proposed phylogeny. It has been shown that accounting for tree topology and branch length uncertainty can provide some level of confidence in the interpretation of the PIC results (Garland et al., 1993; Martins, 1996; Miles and Dunham, 1993; Housworth and Martins, 2001). The use of Mesquite allowed us to assess the sensitivity of the results to variation in tree topology and branch lengths. By testing the correlated evolution of characters using 10 000 phylogenies obtained from a Bayesian analysis, including many unlikely scenarios, we show (Fig. 5) that the character data are strongly correlated within the vast majority of phylogenetic relationships.

Concluding remarks

We have shown that the effect of body mass on metabolic rate during hovering flight in orchid bees can be understood in terms of the scaling of wing kinematics and morphometric parameters. The body mass effect on metabolism during flight in this lineage occurs through the scaling of wing form and wing loading, which in turn determine the scaling of wingbeat frequency and, therefore, metabolic rate. Such results illustrate the linked relationship of form and function in relation to locomotion, as well as the importance of incorporating an integrative approach in studies of whole-animal metabolic rate scaling.

Recently, models have been proposed to explain the allometric scaling of metabolism based on the assumption that metabolic rates are limited by supply rates *via* branching (Banavar et al., 2002) or fractal-like (West et al., 1999) distribution systems. In honey bees, flight metabolism does not appear to be limited by O_2 supply through the tracheal system which, apparently, possesses considerable excess capacity (Harrison et al., 2001; Joos et al., 1997). Although data in this regard are unavailable for orchid bees, our findings suggest that wing form and kinematics, rather than merely supply limitations, are the main determinants of flight metabolic rate and its allometric scaling.

During hovering flight in bees, >90% of the oxygen consumed is accounted for by oxidative metabolism in the flight muscles. Within the flight muscles, most of the ATP hydrolysis that occurs is due to actomyosin ATPase activity, which is activated during high rates of cross-bridge cycling. It

would be of interest to examine the biochemical correlates of metabolic rate scaling in orchid bees, a further dimension in the evolution of form and function in this interesting clade (see accompanying paper, Darveau et al., 2005).

List of symbols and abbreviations

cyt b	cytochrome *b* gene
M_b	body mass
n	wingbeat frequency
Pw	wing loading
PIC	phylogenetically independent contrast
R	forewing length
S	total wing area
$\dot{V}_{CO_2}$	carbon dioxide production rate
$\dot{V}^*_{CO_2}$	mass-specific carbon dioxide production rate
$\dot{V}_{O_2}$	oxygen consumption rate

This work was supported by a NSF research grant (IBN0075817) to R.K.S., a NSERC grant to P.W.H., and predoctoral fellowships from NSERC and FCAR to C.A.D. We thank Patricia Schulte for comments that improved the manuscript, Wayne Maddison for helpful discussion, Daniel Suarez and Sophie Breton for help with *cyt b* amplification, John R. B. Lighton and Barbara Joos for technical advice and assistance, and Jim Childress for donating his Sable Systems CO_2 analyzer to the cause. The indispensable help of Oris Acevedo made the work on Barro Colorado Island possible. This work is dedicated to Peter Hochachka, a truly inspiring mentor and friend.

References

Ascher, J. S. and Danforth, B. N. (2001). Phylogenetic utility of the major opsin in bees (Hymenoptera: apoidea): a reassessment. *Mol. Phylogenet. Evol.* **19**, 76-93.

Banavar, J. R., Maritan, A. and Rinaldo, A. (1999). Size and form in efficient transportation networks. *Nature* **399**, 130-132.

Byrne, D. N., Buchmann, S. L. and Spangler, H. G. (1988). Relationship between wing loading, wingbeat frequency and body mass in homopterous insects. *J. Exp. Biol.* **135**, 9-23.

Cameron, S. A. (2004). Phylogeny and biology of neotropical orchid bees (Euglossini). *Annu. Rev. Entomol.* **49**, 377-404.

Casey, T. M., May, M. L. and Morgan, K. R. (1985). Flight energetics of euglossine bees in relation to morphology and wing stroke frequency. *J. Exp. Biol.* **116**, 271-289.

Crabtree, B. and Newsholme, E. (1972). The activities of phosphorylase, hexokinase, phosphofructokinase, lactate dehydrogenase and the glycerol 3-phosphate dehydrogenase in muscles from vertebrates and invertebrates. *Biochem. J.* **126**, 49-58.

Darveau, C.-A., Hochachka, P. W., Roubik, D. W. and Suarez, R. K. (2005). Allometric scaling of flight energetics in orchid bees: evolution of flux capacities and flux rates. *J. Exp. Biol.* **208**, 3593-3602.

Dick, C., Roubik, D. W., Gruber, K. and Bermingham, E. (2004). Long-distance gene flow and cross-Andean dispersal of lowland rainforest bees (Apidae: Euglossini) revealed by comparative mtDNA phylogeography. *Mol. Ecol.* **13**, 3775-3785.

Dillon, M. E. and Duldey, R. (2004). Allometry of maximum vertical force production during hovering flight of the neotropical orchid bees (Apidae: Euglossini). *J. Exp. Biol.* **207**, 417-425.

Dressler, R. L. (1978). Infra-generic classification of Euglossa, with notes in some features of special taxonomic importance (Hymenoptera, Apidae). *Rev. Biol. Trop.* **26**, 187-198.

Dudley, R. (1995). Extraordinary flight performance of the orchid bees (Apidae: Euglossini) hovering in heliox (80% He/20% O_2). *J. Exp. Biol.* **198**, 1065-1070.

Dudley, R. (2000). *The Biomechanics of Insect Flight: Form, Function, Evolution*. Princeton: Princeton University Press.

Felsenstein, J. (1985). Phylogenies and the comparative method. *Am. Nat.* **125**, 1-15.

Felsenstein, J. (1995). PHYLIP 3.57c: Phylogeny Inference Package. Seattle, WA: The University of Washington.

Garland, T., Jr, Harvey, P. H. and Ives, A. R. (1992). Procedures for the analysis of comparative data using phylogenetically independent contrasts. *Syst. Biol.* **41**, 18-32.

Garland, T., Jr, Dickerman, A. W., Janis, C. M. and Jones, J. A. (1993). Phylogenetic analysis of covariance by computer simulation. *Syst. Biol.* **42**, 265-292.

Harrison, J. F., Camazine, S., Marden, J. H., Kirkton, S. D., Rozo, A. and Yang, X. L. (2001). Mite not make it home: tracheal mites reduce the safety margin for oxygen delivery of flying honeybees. *J. Exp. Biol.* **204**, 805-814.

Harvey, P. H. and Pagel, M. D. (1991). *The Comparative Method in Evolutionary Biology*. Oxford: Oxford University Press.

Housworth, E. A. and Martins, E. P. (2001). Conducting phylogenetic analyses when the phylogeny is partially known: Random sampling of constrained phylogenies. *Syst. Biol.* **50**, 628-639.

Huelsenbeck, J. P. and Ronquist, F. (2001). MrBayes: bayesian inference of phylogeny. *Bioinformatics* **17**, 754-755.

Joos, B., Lighton, J. R., Harrison, J. F., Suarez, R. K. and Roberts, S. P. (1997). Effects of ambient oxygen tension on flight performance, metabolism, and water loss of the honeybee. *Physiol. Zool.* **70**, 167-174.

Koulianos, S. and Schmid-Hempel, P. (2000). Phylogenetic relationship among bumble bees (Bombus, Latreille) inferred from mitochondrial cytochrome b and cytochrome oxidase I sequences. *Mol. Phylogenet. Evol.* **14**, 335-341.

Kumar, S., Tamura, K., Jakobsen, I. B. and Nei, M. (2001). MEGA2: molecular evolutionary genetics analysis software. *Bioinformatics* **17**, 1244-1245.

Maddison, W. P. and Maddison, D. R. (2004). Mesquite: A modular system for evolutionary analysis. Version 1.02. http://mesquiteproject.org.

Martins, E. P. (1996). Conducting phylogenetic comparative studies when the phylogeny is not known. *Evolution* **50**, 12-22.

Martins, E. P. and Housworth, E. A. (2002). Phylogeny shape and the phylogenetic comparative method. *Syst. Biol.* **51**, 873-880.

Michel-Saltzat, A., Cameron, S. A. and Oliveira, M. L. (2004). Phylogeny of the orchid bees (Hymenoptera: Apinae; Euglossini): DNA and morphology yield equivalent patterns. *Mol. Phylogenet. Evol.* **32**, 309-323.

Midford, P. E., Garland, T., Jr and Maddison, W. P. (2003). PDAP Package.

Miles, D. B. and Dunham, A. E. (1993). Historical perspectives in ecology and evolutionary biology: The use of phylogenetic comparative analyses. *Ann. Rev. Ecol. Syst.* **24**, 587-619.

Pennycuick, C. and Rezende, M. (1984). The specific power output of aerobic muscle, related to the power density of mitochondria. *J. Exp. Biol.* **108**, 377-392.

Rothe, U. and Natchigall, W. (1989). Flight of the honeybee. IV. Respiratory quotients and metabolic rate during sitting, walking, flying. *J. Comp. Physiol.* **158**. 739-749.

Roubik, D. W. and Hanson, P. E. (2004). *Orchid Bees of Tropical America: Biology and Field Guide.* Costa Rica: Editorial INBio.

Saktor, B. (1976). Biochemical adaptations for flight in the insect. *Biochem. Soc. Symp.* **41**, 111-131.

Sotavalta, O. (1952). The essential factor regulating the wing-stroke frequency of insects in wing mutilation and loading experiments and in experiments at subatmospheric pressure. *Ann. Zool. Soc. Vanamo* **15**, 1-67.

Suarez, R. K. (2000). Energy metabolism during insect flight: biochemical design and physiological performance. *Physiol. Biochem. Zool.* **73**, 765-771.

Suarez, R. K., Darveau, C.-A., Welch, K. C., Jr, O'Brien, D. M., Roubik, D. W. and Hochachka, P. W. (2005). Energy metabolism in orchid bee flight muscles: carbohydrate fuels all. *J. Exp. Biol.* **208**, 3573-3579.

West, G. B., Brown, J. H. and Enquist, B. J. (1999). The fourth dimension of life: fractal geometry and allometric scaling of organisms. *Science* **284**, 1677-1679.